ADVANCED BIOSYSTEMS
www.adv-biosys.com

Paper-Based Cell Cryopreservation

*Roaa Alnemari, Pavithra Sukumar, Muhammedin Deliorman, and Mohammad A. Qasaimeh**

The continuous development of simple and practical cell cryopreservation methods is of great importance to a variety of sectors, especially when considering the efficient short- and long-term storage of cells and their transportation. Although the overall success of such methods has been increased in recent years, there is still need for a unified platform that is highly suitable for efficient cryogenic storage of cells in addition to their easy-to-manage retrieval. Here, a paper-based cell cryopreservation method as an alternative to conventional cryopreservation methods is presented. The method is space-saving, cost-effective, simple and easy to manage, and requires no additional fine-tuning to conventional freezing and thawing procedures to yield comparable recovery of viable cells. It is shown that treating papers with fibronectin solution enhances the release of viable cells post thawing as compared to untreated paper platforms. Additionally, upon release, the remaining cells within the paper lead to the formation and growth of spheroid-like structures. Moreover, it is demonstrated that the developed method works with paper-based 3D cultures, where preformed 3D cultures can be efficiently cryopreserved.

1. Introduction

Successful preservation of cells is extremely critical for their storage, transportation, and distribution. Conventional cryopreservation methods, such as slow freezing and vitrification, need to be precise and reliable so that cells can be used, directly or indirectly, at future times. Hence, the main goal of these methods is to put the cells, with minimal injuries, in a state where cells' metabolic activities "freeze." Among them, slow freezing has been commonly used for preserving cells for over 70 years.[1,2] The principle of the method involves freezing the cells slowly (up to 2 h) to sub-zero temperatures so that their metabolic activities are paused during their storage. As a result, the use of low concentration cryoprotectants and slow cooling in this method enables high cell viability and sustainable cell characteristics for various sample types, including embryos, sperms, oocytes, and primary cells and cell lines.[3–5] However, the method efficacy is considerably poor for complex multilayered samples, such as organoids, cell–scaffold constructs, and full organs due to samples' inability to completely absorb the cryoprotectants in freezing medium. On the contrary, vitrification utilizes higher concentration of cryoprotectants and expresses rapid cooling (within minutes) as a result of which cells/tissues are preserved in a "glass-like" state.[1,2,6] While both approaches have their merit, in general they commonly suffer from a major limitation: maintaining the broad sample stocks to ensure steady supply.[7–9] As such, to store hundreds of samples in thousands of cryogenic containers requires large-scale units. Consequently, difficulties in managing such vast amount of content contribute to loss, damage, or misidentification of cells/tissues during sample retrievals.[10] For example, the American Type Culture Collection (ATCC, a leading cell line provider), nowadays maintains over 4000 different types of cell lines. Based on a 1996 report,[11] where the ATCC was estimated to manage their cell lines in about half a million cryotubes, we are expecting that tens of millions of cryotubes are being stored around the world.

Therefore, an increased amount of efforts have been made to overcome the long-term preservation challenges for simple-to-complex samples and allowing easy and affordable access to different type of cells and tissues in a timely manner.[12–18] Notably, when coupled with the ongoing continuous demand for cryopreservation of 3D cell cultures in more natural settings, scaffolds with varying pore sizes have seemed to provide a good route to pursue a successful cryogenic storage of cells through the use of conventional cryopreservation methods.

3D cell cultures are a demanding technology where cells are allowed to grow within scaffolds so that cell–cell/cell–environment interactions are possible; thus mimicking in vivo tissue microenvironment. To date, various substrates, such as glass, metals, polymers, hydrogels, and paper, have been utilized as scaffolds to match the microenvironment of the cells/tissues of interest.[19] Among them, paper has become an attractive platform in tissue engineering development, and especially in 3D cell culture, offering remarkable features including biocompatibility, porosity, cost-effectiveness, and applicability

R. Alnemari, P. Sukumar, Dr. M. Deliorman, Prof. M. A. Qasaimeh
Division of Engineering
New York University Abu Dhabi (NYUAD)
Abu Dhabi 129188, UAE
E-mail: mohammad.qasaimeh@nyu.edu
Prof. M. A. Qasaimeh
Department of Mechanical and Aerospace Engineering
New York University
Brooklyn, NY 11201, USA
The ORCID identification number(s) for the author(s) of this article can be found under https://doi.org/10.1002/adbi.201900203.

DOI: 10.1002/adbi.201900203

for large-scale biological testing and microfabrication due to its tunable surface characteristics.[20–23] In addition, paper platforms were previously used as vitrification containers to enhance cryopreservation of mouse embryos[24] and bovine matured oocytes[25] and blastocysts.[26] Indeed, results of these studies revealed that the containers (2D paper surfaces) offer enhanced survival rates of embryos, oocytes, and blastocysts after vitrification compared to conventional cryopreservation. The aim of using the paper container was to take advantage of its high absorbing rates so that the volume of vitrification solution is minimized and rapid cooling/warming is achieved during vitrification/devitrification processes. For preserving tissue constructs, on the other hand, several studies developed engineered porous scaffolds for cryopreservation of precultured cells, such as corn starch–polycaprolactone fiber meshes for mesenchymal stromal cells,[8] electrospun–polyurethane nanofiber sheets for myoblast cells,[27] alginate–gelatin cryogel sponges for stem cells,[9] and reticulated polyvinyl formal resins for fibroblasts.[28] Results of these studies indicated that such scaffolds offer highly protective environment for the retention of cells' viability and content during the cryopreservation. This was attributed to the biocompatibility and mechanical strength of materials from which the scaffolds were made of, along with the porosity that facilitated the uniform distribution of cryoprotectants to the cells at different locations within scaffolds. Cumulatively, however, these scaffolds are needed to be repeatedly manufactured (i.e., engineered) for their use in relevance to cryopreservation of cells. Additionally, their applicability to cryopreserve intact (i.e., non-cultured) cells has not been reported yet. Paper, on the contrary, is ready-to-use scaffold that offers superior compatibility with the cryopreservation in addition to its remarkable potential as a 3D cell culture platform. However, it has never been utilized as a platform to cryopreserve cells.

Here, we describe a method to efficiently cryopreserve cells on paper platforms using standard slow freezing procedures, herein referred to as paper-based cryopreservation (**Figure 1**a). The method is space-saving, cost-effective, simple and easy to manage, and requires no additional modification to the conventional protocols for freezing and thawing cells. In this method, cells are ubiquitous in the 3D porous environment of the paper, where paper fibers provide a natural protective and supportive environment during their cryopreservation. As a result, after their freeze, thawed cells are efficiently released from paper with high viability rates by gently shaking the paper. In addition, preliminary results suggest that the remaining cells residing within the paper can be further utilized to create 3D cell constructs and that the method enables the cryopreservation of paper-based 3D cell culture systems.

The developed method brings several advantages to the field of cell cryopreservation including high viability of preserved cells (comparable to conventional slow freezing method), mechanical stability of paper (platforms with large areas can be rolled and stored in stocks), efficient retrieve/transport of cryopreserved cells in an on-demand manner in small pieces (without a need to thaw the entire platform), and a versatile 3D porous environment tailoring spheroid formations and allowing cryopreservation of precultured cells in 3D. Our main motivation is to provide practical solution for the effective preservation of cells that is space-saving, cost-effective, simple, and easy to manage.

2. Results

2.1. Characterization of Cell Release after Thawing

During the development of the paper-based cell cryopreservation, it was important to recognize that the method does not jeopardize the viability and functions of cells during their load, freeze, and storage while allowing their release from papers after thaw. Therefore, a concern was directed toward the evaporation of water from the paper during the cell loading process. By measuring the change in the water mass within the paper at increasing evaporation times at room temperature, we obtained that the water evaporation rate is 0.002 g min^{-1} per 9 cm^2 paper strip (Figure S1a, Supporting Information). This result suggested that ≈1% of the water mass is evaporated from the paper during the 1 min cell loading, where no harm is expected to the loaded cells. Our next concern was directed toward obtaining effective means to release viable cells from the paper after cryopreservation. Previously, it was reported that fibronectin, a widely used substrate in cell culturing, not only provides a biocompatible surface for the cells to retain their viability but also favors their detachment under shear.[29] With this in mind, we investigated whether fibronectin influences the release of cells from paper upon cryopreservation by comparing the remaining cells on the fibronectin-treated papers to untreated ones after thawing and shaking. To this end, paper fibers were coated with fibronectin at 10 μg mL^{-1} concentration and HeLa (a human cervical cancer cell line) cells were loaded onto papers in the order of ≈10^7 cells per cm^2 of paper strips (Figure 1b), where additional microscopy investigation for the cell loss/damage during paper rolling and insertion inside/removal from cryotubes revealed no significant cell loss/damage within the papers. Results suggested that fibronectin-treated papers substantially enhance the release of viable cells after thawing; a ≈50% increase when compared to untreated papers (Figure 1c,d). Next, to investigate the involvement of fibronectin-coated fibers in the release efficiency of cells and to understand if there are any biological interactions involved, we repeated the same experiments with fluorescently labeled beads having nominal size of 20 μm. As shown in Figure S1b–d, Supporting Information, fibronectin enhanced the release of the loaded beads, while scanning electron microscope (SEM) images of loaded papers confirmed that beads were physically immersed within the 3D environment of the paper (Figure 1e).

To determine whether higher fibronectin concentrations would result in more released cells, additional HeLa cells were loaded onto papers treated with 20 and 30 μg mL^{-1} fibronectin solutions at ≈10^7 cells per cm^2 paper strips. This, however, resulted in slightly higher released cells (58.5% and 55.5%, respectively) in comparison with their release from untreated papers (Figure 1f), suggesting that 10 μg mL^{-1} fibronectin concentration was sufficient for effective release of viable cells from papers following their cryopreservation steps (Figure S2, Supporting Information).

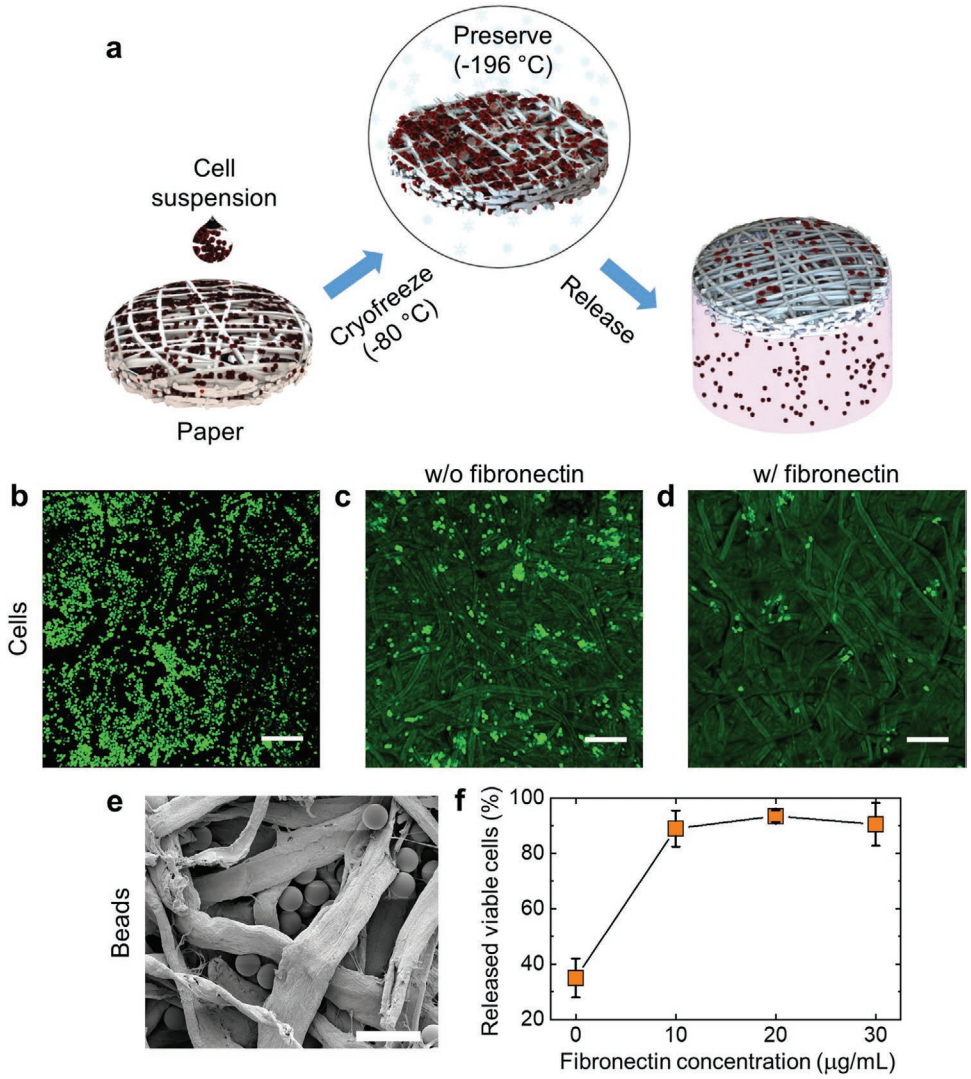

Figure 1. Paper-based cell cryopreservation. a) The methodology for utilizing paper in cryopreservation of cells is simple and robust, allowing for easy loading and efficient freezing of cells. Following their release after freezing, the remaining cells within the paper can be further grown and utilized as in vitro 3D cell constructs. b–d) z-stack confocal images show the cryopreserved HeLa cells (labelled with green cell tracker) before their release from paper and the relative effect of untreated (i.e., without fibronectin) paper on the HeLa cell release to fibronectin-treated one. Scale bar in (b) is 100 μm and in (c) and (d) is 200 μm. e) SEM image shows entrapped beads within a paper, wherein they reveal the interaction of cells with the fibers and their spread in porous 3D microenvironment of the paper. Scale bar is 50 μm. f) The graph represents the release efficiency of viable HeLa cells as a function of fibronectin concentration within the paper, where 10 μg mL^{-1} fibronectin solution is sufficient to release viable cells at about 90% efficiency. Values and error bars represent mean ± SD ($n \geq 3$).

2.2. Cell Viability and Proliferation after Thawing and Release

After confirming the enhanced cell release from fibronectin-coated papers and the fibronectin concentration dependency, our next concern was toward testing the compatibility of the method on maintaining cellular functions during the freeze. As opposed to cryopreservation of suspended cells in cryovials, where the distribution of cryoprotectants occurs homogeneously, cryopreservation of cells within 3D porous environment of paper is expected to be more complex since cryoprotectants need to reach cells at various locations deep in the paper.[30] To assess whether the 3D porous medium of the paper provides a suitable environment to cells during their freeze, first we compared the viability of HeLa cells loaded onto papers. In terms of relative number and distribution of viable cells within papers, live/dead assays suggested that treating papers with 10 μg mL^{-1} fibronectin solution did not offer any additional advantage than untreated ones both before and after their freeze (**Figure 2**a–c; Figure S2a,b,e,f, Supporting Information). However, in terms of viable HeLa cell release from paper after thawing, trypan blue exclusion assays verified that fibronectin-treated papers offer superior advantage to untreated ones (Figure 2d). For example, the release efficiency of HeLa cells using untreated paper was about 35%, whereas the viability of released cells reached about 89% from fibronectin-treated papers.

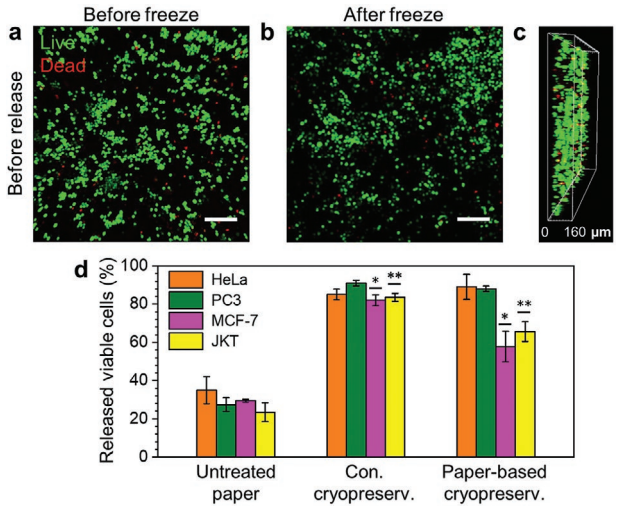

Figure 2. Viability of cells cryopreserved within paper platforms. z-stack confocal images of live (green) and dead (red) HeLa cells within fibronectin-treated papers confirming their unchanged relative numbers a) before and b) after freezing, respectively. Scale bars are 200 µm. c) Side view of the z-stack image in (a) shows the depth distribution of HeLa cells within the paper. d) Trypan blue exclusion assay on HeLa, PC3, MCF-7, and JKT cells reveals that paper-based cryopreservation is comparable to conventional cryopreservation in terms of recovery of viable cells following thawing. * and ** are statistically significant. Values and error bars represent mean ± SD ($n \geq 3$).

Next, to investigate the effectiveness of the method on the release of cells other than HeLa, we conducted additional cell release experiments using PC3 (a human prostate cancer cell line), MCF-7 (a human breast cancer cell line), and JKT (a human T-cell lymphocyte cell line) cells. Regardless of the differences in their sizes and functionalities, overall results suggested that the method efficacy held for PC3, MCF-7, and JKT cells after their release, where no significant difference on cell viability, except for cells loaded on untreated papers, was observed when compared to the conventional cryopreservation (Figure 2d). Similarly, as compared to the outcomes of cells on untreated papers, the release efficiency of PC3, MCF-7, and JKT cells increased by 60.5%, 28.3%, and 42.2%, respectively, when loaded onto 10 µg mL^{-1} fibronectin-treated papers (Figure 2d). These findings were also in agreement with after release live/dead characterization of cells remaining within papers as compared to untreated ones (Figure S2c,d,g,h, Supporting Information). Nonetheless, the release efficiencies of viable MCF-7 and JKT cells from papers were somewhat lower (by 10–15%) than that of recovered cells from conventional cryopreservation. Further investigation of microscopy images of the thawed and released cells revealed that considerable amount of viable cells remains inside the paper (Figure S3, Supporting Information). This could be due to increased focal adhesion sites of these cells[31]—a likely causative factor for reduction in the released viable cells from the paper—and/or their size heterogeneity. Future studies will involve optimizing the release of adherent cells remaining within the paper.

Following live/dead assays, our desire was to investigate the cell activity after thawing and culture by proliferation analysis. Results using HeLa, PC3, MCF-7, and JKT cells indicated no significant differences in the cell morphologies between freshly cultured and thawed cells following their proliferation for up to three consecutive passages with each comprising 3-day measurements. As shown in **Figure 3**a,b, microscopic investigation of filamentous actin (F-actin) and cell nuclei staining did not show any morphological cell abnormality as compared to ones after conventional freezing, including the spreading areas of F-actin and tubulin. WST-1 cell proliferation study was also performed in triplicates for the same group of cells to comparatively quantify the change in relative number of proliferated cells following cell thawing and release. Results confirmed that the confluency of paper-based cryopreserved cells is similar to the conventionally cryopreserved cells (Figure 3c; Figure S4, Supporting Information).

To test if treating papers with fibronectin influences their proliferation after thawing and release, in another set of experiments, we cryopreserved cells in a medium where fibronectin was used as additive. Results suggested that inclusion of fibronectin resulted in similar proliferation of viable cells among cryopreservation methods (Figure S5, Supporting Information).

2.3. Formation of 3D Spheroids

Formation of 3D tumor spheroids has become an attractive pursuit to develop and study anti-cancer drugs. As a result, various methods, such as pellet culture, liquid overlay, hanging liquid drop, and droplet-based microfluidics, have been proven to successfully facilitate easy formation of well-defined spheroids in laboratory settings.[32] In our work, however, when we allowed remaining 10–20% of cells (HeLa and MCF-7) within paper to grow in a culture medium for up to 6 days following the thaw and release, interestingly, they resulted in "grape-like" spheroid growths.[33,34] Indeed, when the surface morphology of paper fibers was investigated, the fibers exhibited wide range of sizes, and large gaps are shown between the paper interlayers (**Figure 4**a). Hence, forming a suitable 3D structural support for aggregation, preservation of cells, and as it follows, for the growth of cell clusters that resemble spheroid-like structures. Figure 4b,c, shows examples of different 3D spheroid formations of the HeLa cells after their cryopreservation in paper. Following their culture for a period of 6 days, their average length grew either exponentially or linearly (Figure 4d) and was seemingly limited only by the pore sizes of the paper within which they resided. Such spheroid formations were easy to achieve if cells were initially loaded at high concentrations (≈10^7 cells per cm^2 paper strips), although at lower cell concentrations we were also able to observe clusters of cells as shown in Figure 4e and Figure S6a, Supporting Information. Additionally, staining the clusters with E-cadherin antibodies revealed the adherens junctions presence at the sites of cell–cell contacts, suggesting that these clusters are not simply aggregates[35] (Figure S6b, Supporting Information). Finally, these clusters were also well distributed within the paper and residing deep in the paper, where live/dead assays confirmed relatively high cell viability within them (Figure 4f).

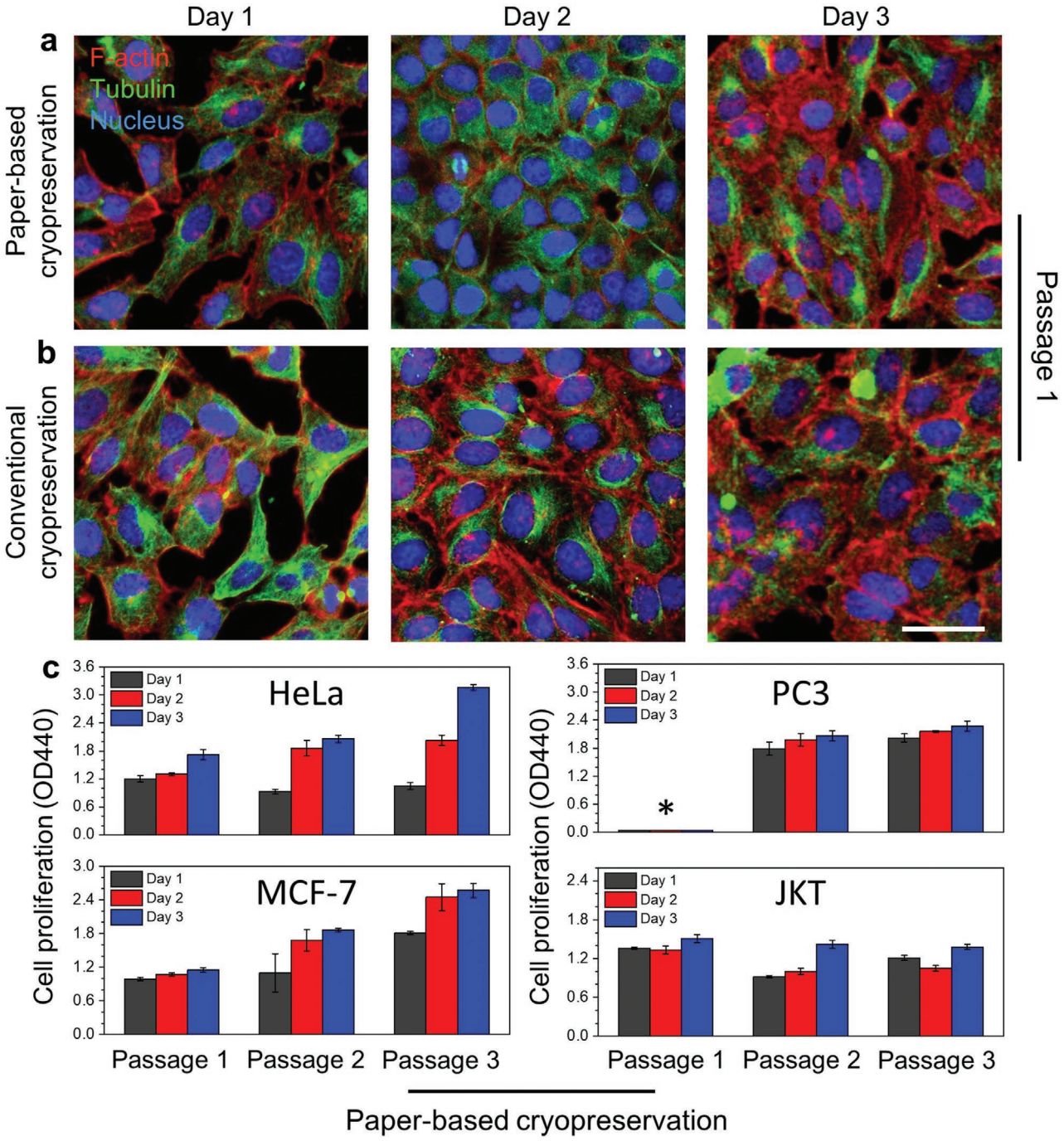

Figure 3. Proliferation of cells cryopreserved within paper platforms. Confocal images show the day 1, day 2, and day 3 proliferation responses of HeLa cells following their a) paper-based and b) conventional cryopreservation. The spread in F-actin (red) and tubulin (green) confirms that paper-based cryopreservation does not hinder the morphology of cells after thawing and release. Nuclei are labelled in blue. Scale bar is 20 µm. e) Optical density measurements on growth of HeLa, PC3, MCF-7, and JKT cells following three consecutive passages for over 3 days reveal that paper-based cryopreservation favors proliferation of released cells after thawing and release. Control experiments are shown in Figure S4, Supporting Information. *, the optical density values are 0.04. Values and error bars represent mean ± SD ($n \geq 3$).

2.4. Cryopreservation of Precultured Cells

After verifying that cells loaded onto papers preserve their viability and functionality during freeze, next we explored whether paper-based cryopreservation will offer a suitable environment for the cryogenic storage of 3D cell culture systems (**Figure 5**a). For this, we investigated its functionality with cells cultured and grown within paper platforms prior

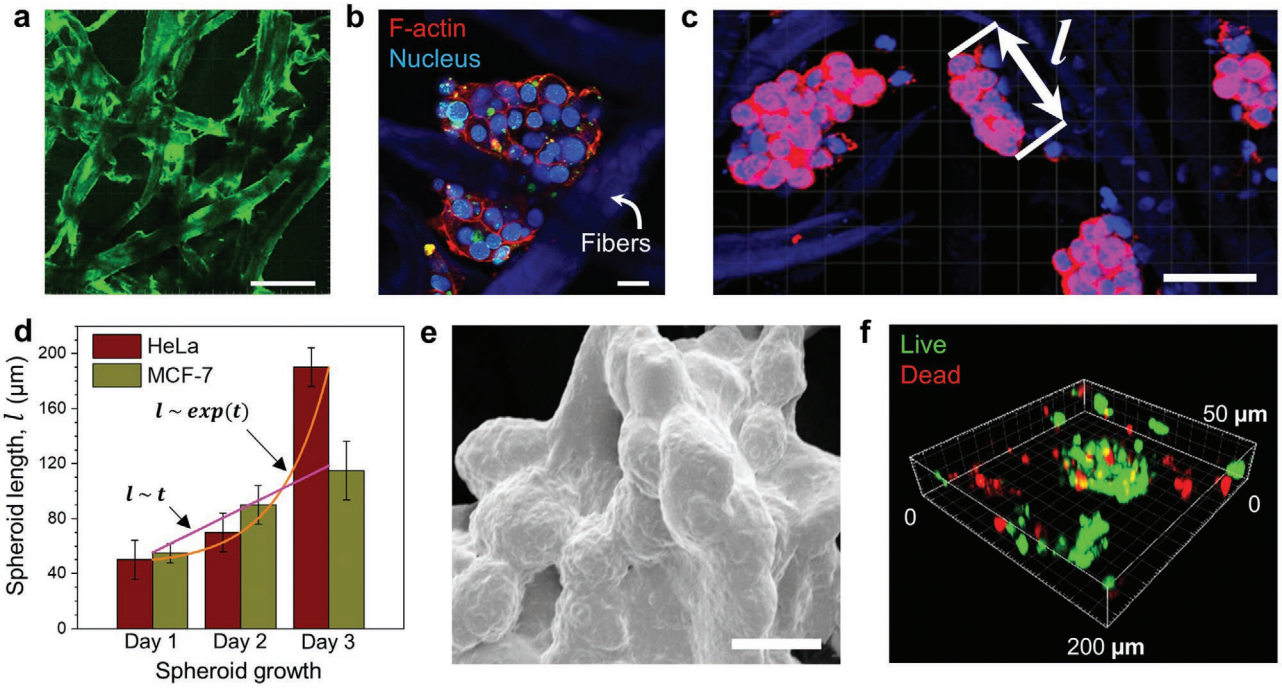

Figure 4. 3D spheroids within the paper platform. a) Confocal image of fibronectin-treated paper reveals fiber coating (green), pore sizes, and 3D interconnectivity of fibers. Scale bar is 100 μm. b) z-stack confocal image shows fairly large spheroid-like structure formed and grown within the paper pores using HeLa cells. Red is F-actin, green is tubulin, and blue is nucleus. Scale bar is 15 μm. c,d) The length *l* of "grape-like" spheroids (Scale bar is 50 μm) was measured to investigate the increase in length of spheroids as a function of culture days for HeLa and MCF-7 cells. Values and error bars represent mean ± SD ($n \geq 3$). e) SEM image shows an example of accumulated cell cluster within a paper pore. Scale bar is 8 μm. f) A 3D confocal image shows the live/dead spatial distribution of the spheroids within paper grown following thawing and cell release.

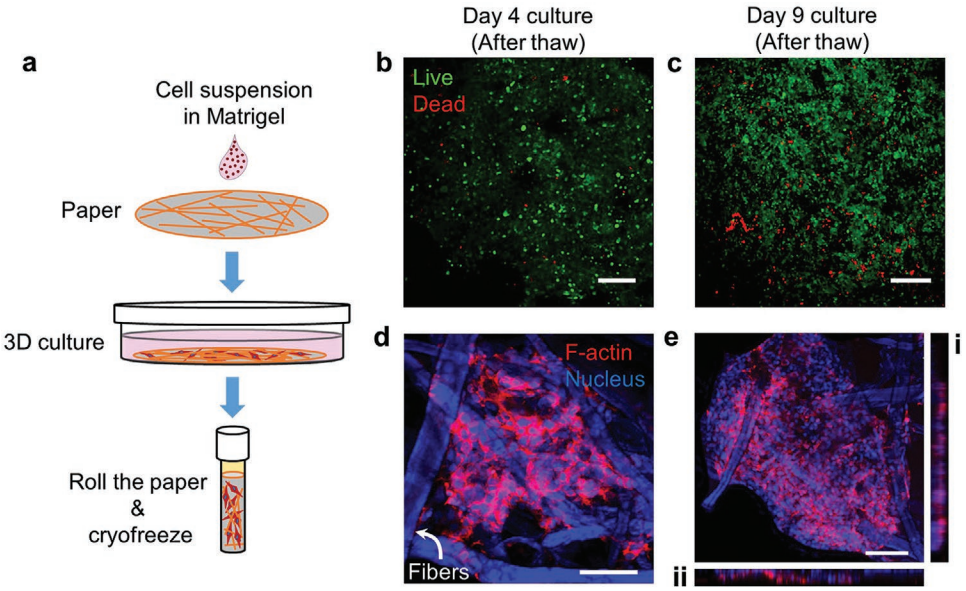

Figure 5. Paper-based cryopreservation of 3D cell cultures. a) Schematic representation of the paper-based cryopreservation method applied to the preservation of precultured cells suspended in Matrigel environment. b,c) Confocal images show the relative distributions of live (green) and dead (red) MCF-7 cells within paper cultured for additional b) 1 day and c) 6 days after their freeze (thawed as day 3), respectively. Scale bars are 100 μm. d,e) z-stack confocal images show the MCF-7 3D cell culture at day 4 and day 9, respectively. Together with the reconstituted z-section images in (i) and (ii), it appears that their growth naturally tends to cover pore spaces and fibers available in their surroundings. Red is F-actin and blue is nucleus. Scale bar in (d) is 50 μm and in (e) is 100 μm.

to their freeze. Matrigel-suspended MCF-7 cells were loaded onto papers at concentrations of ≈10^7 cells per cm^2 paper strips and incubated for 3 days in culture medium (Figure 5b). The paper-based 3D culture was then cryopreserved for 3 days and following thawing, cells (Figure 5c) were additionally cultured for 6 days to fully recover,[8] where their culture medium was replaced once with fresh medium every other day. Overall, our comparative proliferation images at days 4 and 9 showed that the paper-based cryopreservation maintains the integrity and viability of cells precultured before cryopreservation, as confirmed by the uniformly distributed 3D cell layers growing inside the paper (Figure 5d). We then conducted further investigation on the cells' post-cryopreservation 3D spread within the papers. Results showed that the cells' growth tend to fully cover the pore spaces and fibers available in their surroundings (Figure 5e), which corroborated our expectations that the paper-based cryopreservation fully favors the recovery of precultured cells.

3. Discussion

This is the first study to demonstrate that cells can be efficiently cryopreserved within a paper platform as an alternative to conventional cryopreservation methods. In the process of effective cell release after freeze, the significant parameter implicated in paper-based cryopreservation is chemical modification of paper fiber surfaces with fibronectin. For example, our data suggest that 10 μg mL^{-1} fibronectin concentration is sufficient to result in ≈50% increment of released cells compared to untreated fibers alone. Several adhesion assays were developed and used to investigate the rates of cell–substrate bond breakages under controlled detachment forces.[36,37] Common to these assay parameters is the initial attachment time of cells to the flat substrate, which in general defines the amount of cells released as per applied force. As such, short attachment times (<60 min) result in formation of fewer cell–surface bonds because of the round shape of the cells. Hence, when force is applied these bonds are easily dissociated resulting in detachment of cells.[36,38] Taken together, we hypothesize that in our method fibronectin acts more like a lubricant to enhance the cell release from the paper, which is associated with their short-length (<1 min) cell–substrate bond strengths.[29,31,38,39] In addition, we assume that the highly (>50 μm) 3D porous structure of the paper[22,40] also enhances the release of cells upon shear.

Viabilities of released HeLa and PC3 cells in the paper-based cryopreservation were equivalent to ones preserved conventionally; however, MCF-7 and JKT showed lower percentages perhaps due to cell–fiber adhesion. Yet, it is important to emphasize that for cryopreservation of cell lines; practicality, space-saving, and capability of forming 3D cell culture are of great interest, while the absolute numbers of released viable cells can be improved by cutting larger paper strips or increasing the cell concentration at the loading stage.

In agreement with the cell release results, paper-based cell cryopreservation showed no effect on the F-actin and tubulin integrity and organization when compared with non-frozen controls. As main components of the cytoskeleton, these protein structures are known to be very sensitive to any mechanical damage of the cell membrane during cryopreservation.[41] Hence, it is important that the cryopreservation protocol does not cause any disruption in their functionality, particularly resulting from osmotic stresses.[42] Apparently, in our method the random orientation of paper fibers provides protective shield to the cells to withstand the osmotic stresses from the surroundings when they undergo the harsh freezing process. This was also evidenced by a comparative study in which the cell viability after freeze was over two times higher on porous fiber meshes than nonporous disks.[8] Here, we expect that the topography structure of the fibers and porosity of the paper remain intact upon freeze/thaw processes.[8]

In our work, we observed that paper additionally offers—upon the release of cells after thawing—favorable environment for the growth of cell clusters within the paper which result from the remaining cells in paper and resemble 3D spheroid-like structures. Here, due to geometrical complexity of pores in heterogeneous matrices such as paper, the pores that have diameters between 50 and 200 μm have shown to serve as good environment for the growth of the spheroids within the papers. As a result, after 6 days of growth, the average size of HeLa and MCF-7 clusters reached 190 ± 14 μm and 115 ± 21 μm, respectively. The reported cluster structures, when grown as floating culture on a low adhesion plates, or using hanging drops, varies greatly. For example, one study[43] reported that MCF-7 cells can reach a cluster size of 500 μm. It is critical to point that the cluster structure and size depend on initial cell concentration and suspension volume in which they are formed. In our case, the paper porosity may play a factor in cluster growth. However, further investigations are left for future studies. Nevertheless, we hypothesize that the interconnecting fibers serve effectively as "nests" to provide structural support for the spheroid growth deep in the paper, as revealed by scanning electron images and illustrated schematically in Figure S7a,b, Supporting Information, respectively. Finally, our data showed that paper-based cryopreservation promotes the integrity, survival, and viability of cells previously cultured and grown on papers, as evidenced by their strong continuous growth within paper after thawing. As such, following proliferation assays at days 1–3, cells 3D cultured within paper platforms were shown to grow (Figure S8a, Supporting Information). Interestingly, after 7 days of 3D paper-based cell culture, followed by freezing for 2 days at –80 °C, and finally thawing; experiments showed integrity and survival of cells (Figure S8b, Supporting Information). Obviously, and along with previously published reports on various scaffold-based cell cryopreservations,[8,9,27,28] paper-based cryopreservation additionally overcomes the obstacles related to cryopreserving precultured (i.e., adherent) cells on 3D porous environments; namely intracellular crystallization, dehydration injury, mechanical ruptures, and uneven cooling during the freeze.

Putting altogether, we show that the paper will utilize a unique platform for cryopreserving cells, where the fibronectin coating on the fibers and 3D porosity of the paper enhance the performance of cryopreservation in terms of high percentage of released viable cells. This makes the paper-based cryopreservation comparable to conventional cryopreservation. Additionally, the method is space-saving and simple to manage, since large sheets of papers can be rolled or folded during their storage

and cut into small pieces during cells' retrieval without a need to thaw the entire platform. These characteristics of the method are expected to overcome the difficulties associated with storing and managing small cryotubes of cryopreserved cells within large containers in an easy and affordable manner.

Finally, results showed that the paper-based method also promises the cryopreservation of precultured cells and favors the formation and growth of spheroids-like structures from the cells remaining within the paper. These findings suggest that the method could empower the preservation of 3D cell cultures and the large-scale production of spheroids. The latter can be achieved by engineering the paper with patterned hydrophobic and hydrophilic regions so that an array of "virtual" microwells are formed for preferential spheroid formations. This can be expanded even further to wider applications such as stacking the paper sheets on the top of each other to mimic different forms of in vivo 3D tumor models. This way, simultaneous investigation of their complex morphological and physiological characteristics in a single experiment would be possible.

4. Experimental Section

Paper Preparation: Whatman Grade 114 cellulose filter papers (Sigma-Aldrich) were used as platform in cell cryopreservation studies (thermal conductivity ≈0.107 W m^{-1} K^{-1},[44] specific heat capacity = 1256 J kg^{-1} K^{-1},[45] density ≈0.039 g cm^{-3}). After autoclaving, papers (≈190 µm thick) were cut into strips of about 30 mm in length and 30 mm in width. They were then either kept as untreated or submerged in a phosphate buffered saline (PBS) containing 10, 20, and 30 µg mL^{-1} concentrations of fibronectin human plasma (Sigma-Aldrich) for 20 min at room temperature. The excess fibronectin in the latter was removed by washing the papers twice with PBS.

Cell Loading, Freezing, and Thawing: HeLa, MCF-7, PC3, and JKT were obtained from The ATCC and used in this study. They were cultured in sterile T75 tissue culture flasks (Fisher Scientific) using complete Dulbecco's modified essential medium (DMEM) for HeLa and MCF-7 cells and Roswell Park Memorial Institute medium for PC3 and JKT cells, where both media (Gibco) were supplemented with 10% fetal bovine serum (FBS; Sigma-Aldrich) and 1% penicillin–streptomycin (Pen-Strep, Sigma-Aldrich). They were then placed in a humidifying incubator at 37 °C and 5% CO_2. The overall passage numbers varied between 15 and 24 for HeLa cells and between 8 and 15 for PC3, MCF-7, and JKT cells. Then, adherent HeLa, PC3, and MCF-7 cells were dissociated from the flasks when about 80% confluent using TrypLE express enzyme (Gibco) and centrifuged at 300 × *g* for 5 min, while suspended JKT cells were collected and centrifuged at 200 × *g* for 7 min. Following resuspension of cell pellets (≈10^7 cells) in 10% FBS and 80% DMEM freezing medium complemented with 5%, for JKT cells, or 10% dimethyl sulfoxide (DMSO; Sigma-Aldrich), for HeLa, PC3, and MCF-7 cells, 300 µL of cell suspensions were pipetted onto the untreated and fibronectin-treated papers. Immediately after (<1 min), papers were rolled and placed in standard cryotubes so that evaporation of the cell suspension is prevented. 100 µL cell suspension (10^7 cells per mL working concentration) was enough to saturate the 3 × 3 × 0.02 cm^3 paper volume with cells. In parallel, 500 µL of cell suspensions were placed in cryotubes and used as controls. Both sets were then frozen at –80 °C over the course of 24 h and placed in liquid nitrogen bath (–196 °C) for extended storage times, ranging from 3 days to 6 months. Cells loaded onto papers without cryopreservation step were used as control.

For each experiment, cryotubes were taken from liquid nitrogen and frozen cells were thawed in a 37 °C water bath for 30 s. Then, the cells (suspended in freezing medium or loaded in papers) were removed from the cryotubes and resuspended/placed in centrifuge tubes containing 10 mL of warm DMEM medium. To release the cells from paper, the tubes were shaken gently for about 20 s. Then, the cell suspensions were centrifuged and the cell pellets were resuspended in a fresh complete culture medium. Cell counting chamber slides (Invitrogen) and 96-well culture plates (Fisher Scientific) were used for viability and proliferation assays, respectively, as explained in details below. Unless otherwise stated, all assays were repeated twice and performed using triplicate samples.

Cell Viability and Proliferation: After freezing and thawing, live/dead fluorescent cell viability imaging assay (Invitrogen) was used to visually assess (as control) the distribution of live/dead cells (HeLa) within the papers—prior to and after their release—using confocal microscopy. Meanwhile, in parallel released cells from papers were removed from DMEM medium and washed three times with PBS. Following their resuspension in fresh culture medium, trypan blue exclusion assay (Sigma-Aldrich) was applied to directly count the number of released live and dead cells using Countess II FL (Fisher Scientific) automated cell counter and their averaged proportions were converted to percentages and recorded as bar charts for comparison.

WST-1 test (Sigma-Aldrich) was used to quantify the proliferation of released cells. Here, cells were seeded in 96-well culture plates at concentrations of ≈10^4 cells mL^{-1} per well for 3 days following three consecutive passages and WST-1 was performed at days 1, 2, and 3 for each passage. Following their incubations at 37 °C and 5% CO_2, at each day, Varioskan Flash plate reader (Fisher Scientific) was used to determine the cell growth by measuring the changes in the optical densities at 440 nm (OD440) in correlation with the confluence of proliferated cells. In parallel, the background was measured at OD640 and subtracted from each OD440 measurement. Then, the mean OD values were compared to the proliferation of cells cryopreserved using conventional method, with and without fibronectin as additive to cryopreservation medium, and recorded as bar charts.

Following the proliferation measurements, cells were fixed with paraformaldehyde (Sigma-Aldrich) in PBS (2% v/v) for 10 min at room temperature and permeabilized with Triton X-100 (Sigma-Aldrich) in PBS (0.5% v/v) for 15 min. Then, bovine serum albumin (Sigma-Aldrich) in PBS (1% v/v) was used for 20 min to block any non-specific staining. After blocking, F-actin, tubulin, and nuclei staining was done using rhodamine phalloidin conjugated to red-orange fluorescent dye (Cytoskeleton), anti-Alpha tubulin antibodies conjugated to green dye (Abcam), and Hoechst 33342 conjugated to blue dye (Invitrogen), respectively, for 20 min at room temperature in the dark. Finally, their images were taken using confocal microscopy. As a result, the morphological changes in their structures were visually examined and compared with the proliferation response of conventionally cryopreserved cells.

Spheroid Formation and Size Evaluation: After thaw/release process, the papers were resubmerged in a complete culture medium (DMEM supplemented with 10% FBS and 1% Pen-Strep) and incubated at 37 °C and 5% CO_2 for 3 days. After every other day, live/dead assays were performed to visually verify the viability of the spheroids as control. In parallel, after washing papers gently with PBS, cells were stained for F-actin, tubulin, and nuclei for 20 min at room temperature in the dark following the procedure explained in previous section. Then, the papers were mounted on microscopy slides, with their top or bottom sides facing down, using a drop of mounting medium (Vectashield) and left at 4 °C for overnight. Finally, the cells within the papers were imaged using confocal and scanning electron microscopy, as explained in detail in the imaging section.

The size evaluation of spheroids was carried out by measuring their apparent length in the projection of z-stack images. HeLa and MCF-7 cells were used as model. With 2–3 spheroids per measurement, the spheroid lengths following their growth at days 1, 3, and 6 were measured and their mean values were recorded as bar charts.

Precultured Cell Preservation: HeLa and MCF-7 cells (≈10^7 cells per mL) were added to 100% Matrigel (Sigma-Aldrich) at 4 °C (placed in ice) and subsequently their cell suspensions in Matrigel were pipetted onto the papers.[22] Then, papers were left for 10 min at room temperature for the Matrigel to solidify. Following, papers were submerged in a complete culture medium for 3 days at 37 °C and 5% CO_2 to allow the proliferation

of cells. Then, papers were washed three times in PBS, rolled and placed in standard cryotubes containing DMEM freezing medium and frozen at −80 °C for overnight. After their preservation at −196 °C for 3 days, cells were thawed, and papers were removed from the cryotubes and resuspended in complete culture medium for additional 8-day cell proliferation. Then, cells were fixed and stained for F-actin and nucleus following the methodology explained before. Finally, they were imaged using confocal microscopy.

Scanning Electron and Confocal Microscopy Imaging: Cambridge S360 SEM (Leica) was used to image the cells and beads (Fisher Scientific) within the papers at 5 kV accelerating voltage. The images were acquired digitally using UltraScan software (UltraScan Project). Prior to the imaging, cells were fixed in paraformaldehyde in PBS (2% v/v) for 10 min, dehydrated using increasing concentrations (from 20% to 100%) of ethanol solutions and left to air dry overnight at room temperature. Imaging was carried with coating samples with conductive layer.

Confocal microscopy imaging of cells was carried with FV1000 inverted confocal laser scanning microscope (Olympus) using blue (405 nm), green (488 nm), and red (612 nm) excitation wavelengths. 10× air objective lens was used to image up to 160 µm deep in paper. The z-stack imaging was performed in 5 µm increments and their 3D projections were created using Imaris software (Bitplane).

Statistical Analysis: Statistical analysis was performed with Origin software (OriginLab) using two-way analysis of variance to evaluate differences between viability of released cells after their cryopreservation using paper and conventional methods. A value of $p < 0.05$ was considered statistically significant. Values and error bars represent mean ± SD of at least triplicate experiments.

Supporting Information

Supporting Information is available from the Wiley Online Library or from the author.

Acknowledgements

P.S. and M.D. contributed equally to this work. This study was financially supported by NYU Abu Dhabi (NYUAD). The authors thank Mrs. Christina Johnson for scientific illustration, Dr. Rachid Rezgui for technical assistance, and Dr. Michael Davis for technical discussion. The authors acknowledge the technical support from Core Technology Platforms at NYU Abu Dhabi.

Conflict of Interest

The authors declare no conflict of interest.

Keywords

3D culture, cryopreservation, mammalian cells, paper, spheroids

Received: August 22, 2019
Revised: December 6, 2019
Published online:

[1] D. E. Pegg, *Semin. Reprod. Med.* **2002**, *20*, 005.
[2] J. G. Baust, D. Y. Gao, J. M. Baust, *Organogenesis* **2009**, *5*, 90.
[3] T. H. Jang, S. C. Park, J. H. Yang, J. Y. Kim, J. H. Seok, U. S. Park, C. W. Choi, S. R. Lee, J. Han, *Integr. Med. Res.* **2017**, *6*, 12.
[4] J. U. Hermansen, G. E. Tjonnfjord, L. A. Munthe, K. Tasken, S. S. Skanland, *Sci. Rep.* **2018**, *8*, 17651.
[5] G. N. Stacey, J. R. Masters, *Nat. Protoc.* **2008**, *3*, 1981.
[6] P. Bruggeller, E. Mayer, *Nature* **1980**, *288*, 569.
[7] J. O. M. Karlsson, M. Toner, *Biomaterials* **1996**, *17*, 243.
[8] P. F. Costa, A. F. Dias, R. L. Reis, M. E. Gomes, *Tissue Eng., Part C* **2012**, *18*, 852.
[9] A. Katsen-Globa, I. Meiser, Y. A. Petrenko, R. V. Ivanov, V. I. Lozinsky, H. Zimmermann, A. Y. Petrenko, *J. Mater. Sci.: Mater. Med.* **2014**, *25*, 857.
[10] M. Tomlinson, *Hum. Reprod.* **2005**, *20*, 1751.
[11] *Resource Sharing in Biomedical Research* (Eds: F. J. Manning, E. C. Bond, K. I. Berns), The National Academies Press, Washington, DC **1996**.
[12] G. Vajta, M. Kuwayama, *Theriogenology* **2006**, *65*, 236.
[13] E. J. Woods, A. Bagchi, W. S. Goebel, R. Nase, V. D. Vilivalam, *Regener. Med.* **2010**, *5*, 659.
[14] W. H. Shih, Z. Y. Yu, W. T. Wu, *Cryobiology* **2013**, *67*, 280.
[15] E. Puschmann, C. Selden, S. Butler, B. Fuller, *Cryobiology* **2017**, *76*, 65.
[16] N. E. Vrana, K. Matsumura, S. H. Hyon, L. M. Geever, J. E. Kennedy, J. G. Lyons, C. L. Higginbotham, P. A. Cahill, G. B. McGuinness, *J. Tissue Eng. Regener. Med.* **2012**, *6*, 280.
[17] J. Kumari, A. Kumar, *Sci. Rep.* **2017**, *7*, 41551.
[18] J. Y. Lee, Y. Koo, G. Kim, *ACS Appl. Mater. Interfaces* **2018**, *10*, 9257.
[19] D. Lantigua, Y. N. Kelly, B. Unal, G. Camci-Unal, *Adv. Healthcare Mater.* **2017**, *6*, 1700619.
[20] X. C. Wu, S. Suvarnapathaki, K. Walsh, G. Camci-Unal, *MRS Commun.* **2018**, *8*, 1.
[21] K. Ng, B. Gao, K. W. Yong, Y. H. Li, M. Shi, X. Zhao, Z. D. Li, X. H. Zhang, B. Pingguan-Murphy, H. Yang, F. Xu, *Mater. Today* **2017**, *20*, 32.
[22] R. Derda, A. Laromaine, A. Mammoto, S. K. Y. Tang, T. Mammoto, D. E. Ingber, G. M. Whitesides, *Proc. Natl. Acad. Sci. U. S. A.* **2009**, *106*, 18457.
[23] R. Derda, S. K. Y. Tang, A. Laromaine, B. Mosadegh, E. Hong, M. Mwangi, A. Mammoto, D. E. Ingber, G. M. Whitesides, *PLoS One* **2011**, *6*, e18940.
[24] A. K. Paul, Y. Y. Liang, K. Srirattana, T. Nagai, R. Parnpai, *Anim. Sci. J.* **2018**, *89*, 307.
[25] Y. M. Kim, S. J. Uhm, M. K. Gupta, J. S. Yang, J. G. Lim, Z. C. Das, Y. T. Heo, H. J. Chung, I. K. Kong, N. H. Kim, H. T. Lee, D. H. Ko, *Theriogenology* **2012**, *78*, 1085.
[26] K. H. Lee, J. C. Sun, C. K. Chuang, S. F. Guo, C. F. Tu, J. C. Ju, *Cryobiology* **2013**, *66*, 311.
[27] O. Batnyam, S. Suye, S. Fujita, *RSC Adv.* **2017**, *7*, 51264.
[28] H. Miyoshi, T. Ehashi, N. Ohshima, A. Jagawa, *Artif. Organs* **2010**, *34*, 609.
[29] A. J. Engler, M. Chan, D. Boettiger, J. E. Schwarzbauer, *J. Cell Sci.* **2009**, *122*, 1647.
[30] I. Bernemann, N. Manuchehrabadi, R. Spindler, J. Choi, W. F. Wolkers, J. C. Bischof, B. Glasmacher, *CryoLetters* **2010**, *31*, 493.
[31] J. E. Schwarzbauer, D. W. DeSimone, *Cold Spring Harbor Perspect. Biol.* **2011**, *3*, a005041.
[32] R. K. Vadivelu, H. Kamble, M. J. A. Shiddiky, N. T. Nguyen, *Micromachines* **2017**, *8*, 94.
[33] P. A. Kenny, G. Y. Lee, C. A. Myers, R. M. Neve, J. R. Semeiks, P. T. Spellman, K. Lorenz, E. H. Lee, M. H. Barcellos-Hoff, O. W. Petersen, J. W. Gray, M. J. Bissell, *Mol. Oncol.* **2007**, *1*, 84.
[34] R. Edmondson, J. J. Broglie, A. F. Adcock, L. J. Yang, *Assay Drug Dev. Technol.* **2014**, *12*, 207.
[35] S. Feng, X. R. Duan, P. K. Lo, S. Liu, X. F. Liu, H. X. Chen, Q. Wang, *Integr. Biol.* **2013**, *5*, 768.
[36] A. J. Garcia, N. D. Gallant, *Cell Biochem. Biophys.* **2003**, *39*, 61.

[37] D. W. Zhou, A. J. Garcia, *J. Biomech. Eng.* **2015**, *137*, 020908.
[38] H. Dakhil, H. Do, H. Hubner, A. Wierschem, *Bioprocess Biosyst. Eng.* **2018**, *41*, 353.
[39] R. J. McCoy, F. J. O'Brien, *Tissue Eng., Part B* **2010**, *16*, 587.
[40] M. Axelsson, S. Svensson, *Pattern Anal. Appl.* **2010**, *13*, 159.
[41] J. Tang, T. Saito, *J. Appl. Oral Sci.* **2017**, *25*, 299.
[42] B. L. Liu, J. McGrath, *Acta Biochim. Biophys. Sin.* **2005**, *37*, 814.
[43] H. Kim, C. H. Cho, J. K. Park, *Biomicrofluidics* **2018**, *12*, 044109.
[44] J. Morikawa, T. Hashimoto, *Polym. Int.* **1998**, *45*, 207.
[45] C. H. Heo, H. Cho, Y. K. Yeo, *Korean J. Chem. Eng.* **2011**, *28*, 1651.

ADVANCED BIOSYSTEMS

Supporting Information

for *Adv. Biosys.*, DOI: 10.1002/adbi.201900203

Paper-Based Cell Cryopreservation

*Roaa Alnemari, Pavithra Sukumar, Muhammedin Deliorman, and Mohammad A. Qasaimeh**

Supplementary Information

Paper-based cell cryopreservation

Roaa Alnemari, Pavithra Sukumar[†], Muhammedin Deliorman[†], and Mohammad A. Qasaimeh[*]

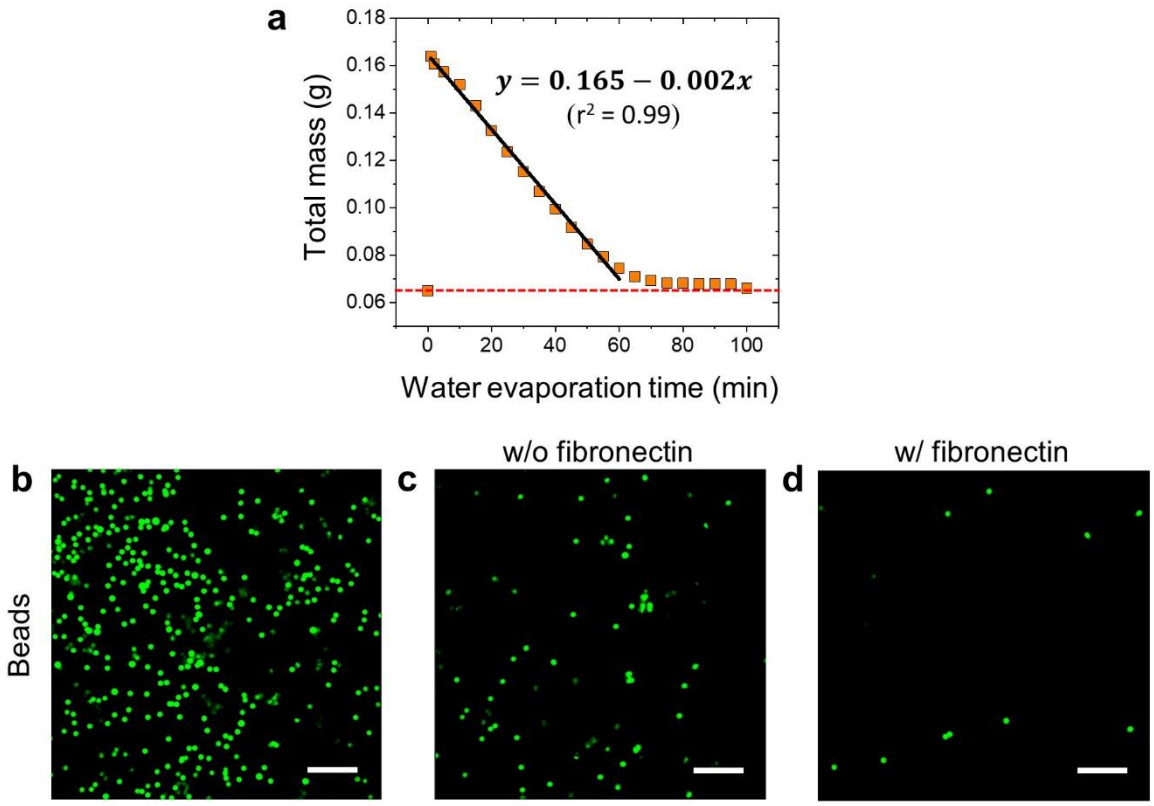

Figure S1. Characterization of water evaporation and bead release. (a) After spotting 100 µL of water onto a 3 × 3 cm^2 paper strip, the change in the water mass within the paper at room temperature was plotted as a function of evaporation time. The water evaporation rate (g min^{-1} per 9 cm^2 paper strips) appeared to decrease linearly until the paper strip is completely dry (red dashed line). (b-d) Confocal images revealed that papers treated with 10 µg/mL concentration of fibronectin favor more release of beads as compared to untreated ones. Scale bars are 200 µm.

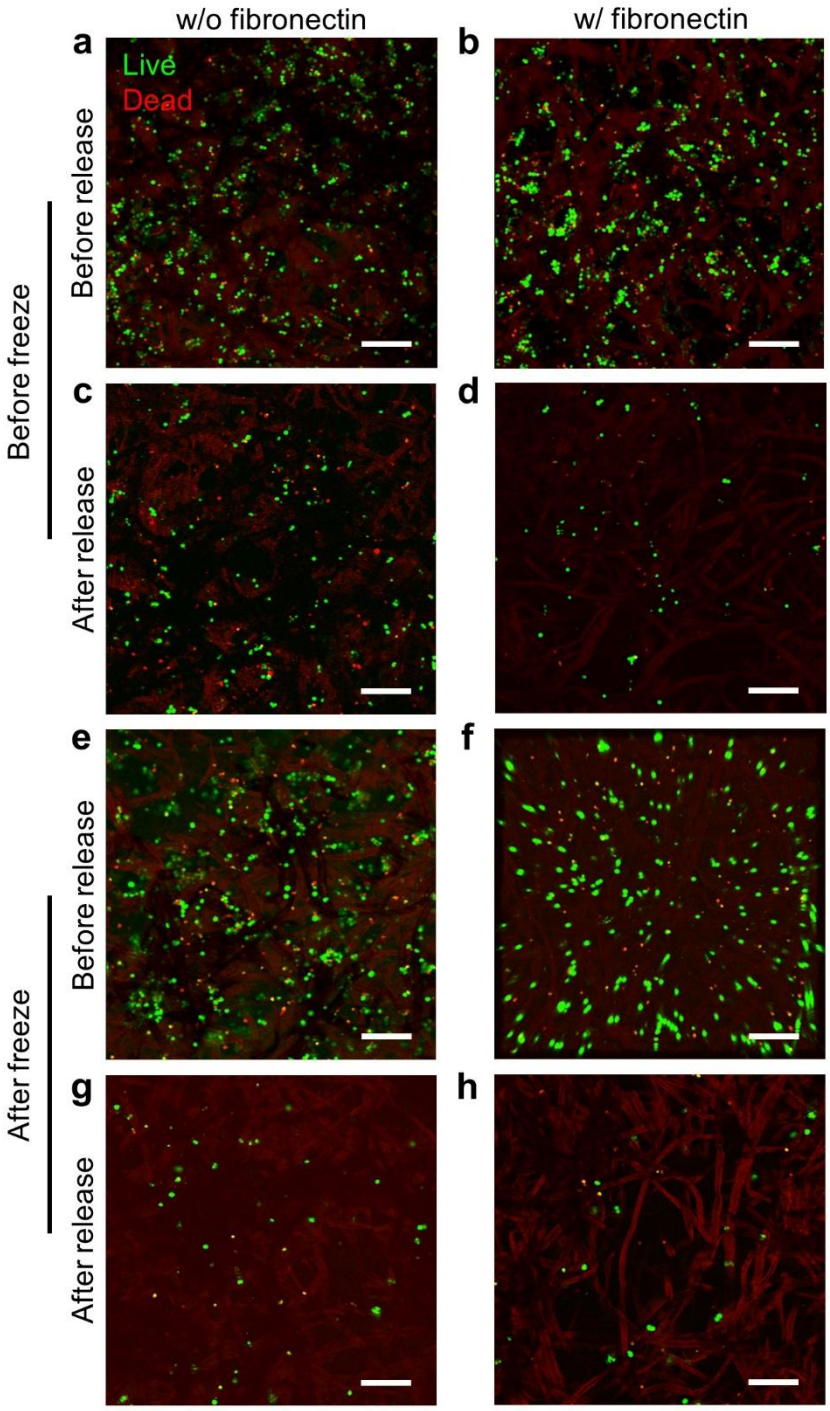

Figure S2. Characterization of cell release. (a-h) Following their load onto untreated and 10 µg/mL fibronectin-treated papers, the relative distribution of live (green) and dead (red) HeLa cells within papers visually showed no difference for (a & b) before and (e & f) after their freeze, respectively. However, investigation of the role of fibronectin in the release of live/dead cells within the papers (c & d) prior to and (g & h) after their freeze confirmed that coating paper fibers with fibronectin enhances the effective release of more viable cells compared to untreated ones. As for the release of dead cells, fibronectin had no apparent effect compared to the non-frozen controls. We hypothesize that in both scenarios (i.e. w/ and w/o fibronectin) the dead cells were more likely entrapped within the 3D fiber network of the paper so that they washed off more easily. Scale bars are 200 µm.

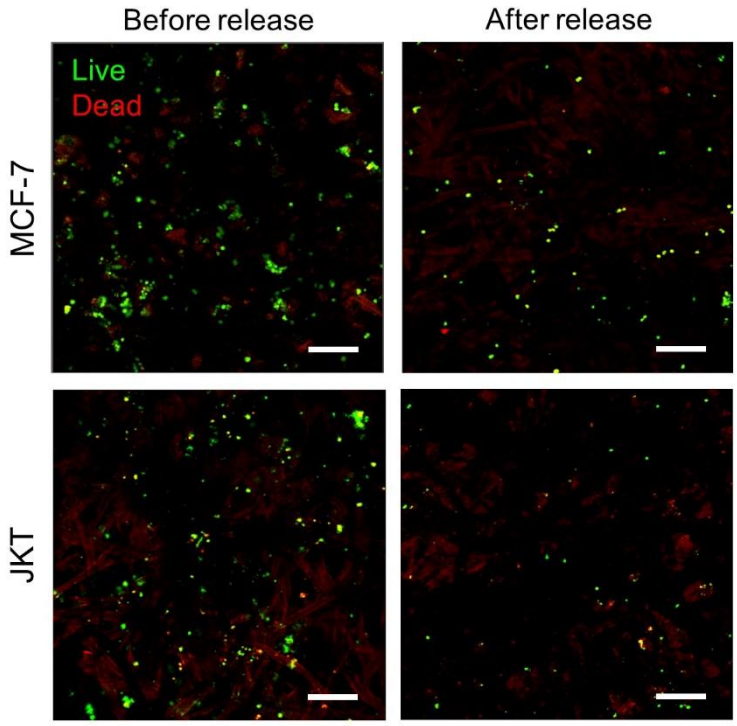

Figure S3. Characterization of viable MCF-7 and JKT release. Investigating the remaining viable MCF-7 and JKT cells within the papers after thawing and release reveals that considerable amount of viable cells remains within the paper, likely due to their strong adhesion to fibronectin-coated paper fibers. Scale bars are 200 µm.

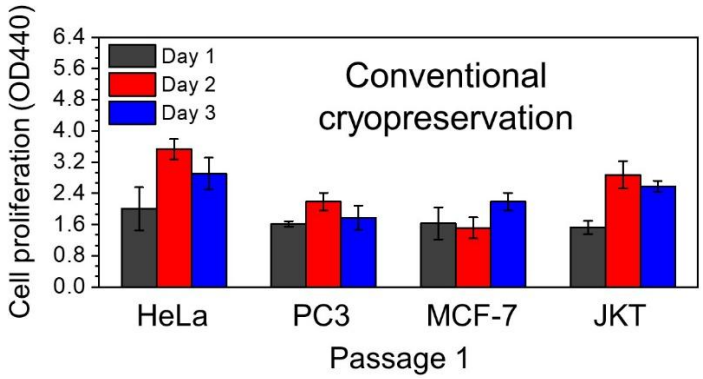

Figure S4. Optical density measurements on HeLa, PC3, MCF-7, and JKT cultures for 3 days after their conventional cryopreservation. These measurements were conducted as control to assess the proliferation of cells released from papers (Figure 3*c*). Values and error bars represent mean ± S.D. ($n \geq 3$).

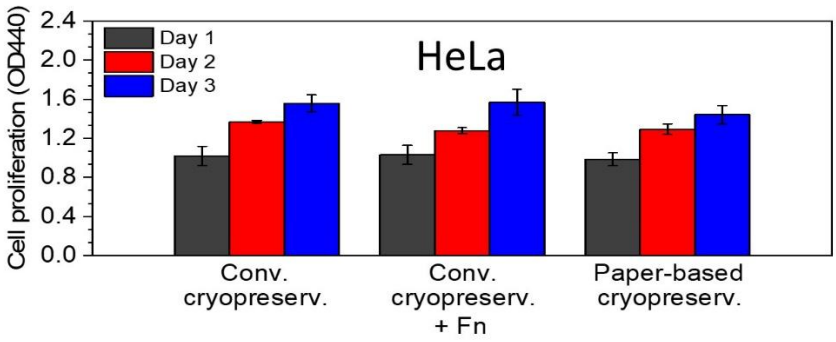

Figure S5. Optical density measurements on proliferated HeLa cells for 3 days after thawing and release reveal that paper-based cryopreservation results in comparable proliferation to conventional cryopreservation. Using fibronectin (F_n) as an additive to the cryopreservation medium did not have an influence on the change in relative numbers of proliferated cells. Values and error bars represent mean ± S.D. ($n \geq 3$).

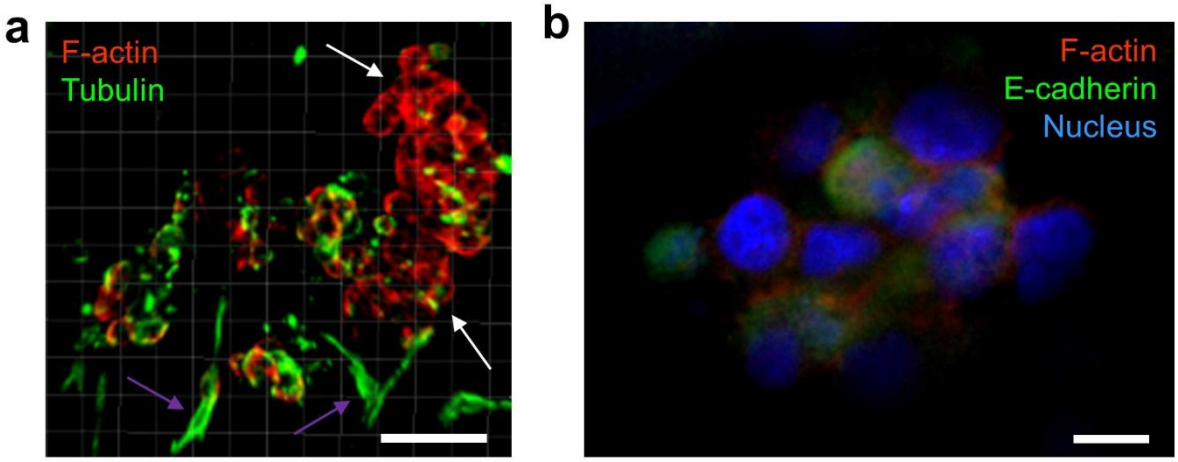

Figure S6. Multiple 3D cell formations within paper. (a) Z-stack confocal image reveals the formation of 3D cell cultures (purple arrows) and spheroids (white arrows) of cryopreserved HeLa cells after their culture for 1 day. The tubulin appeared to be more extended in 3D cell cultures, whereas the F-actin was more condensed in spheroids. These formations were observed when low concentrations ($<10^7$ cells/mL) of cells were loaded onto papers prior to cryofreeze. Scale bar is 80 µm. (b) Staining of HeLa spheroids with E-cadherin antibodies reveals the presence of adherens junctions at sites of cell-cell contacts. Scale bar is 10 µm.

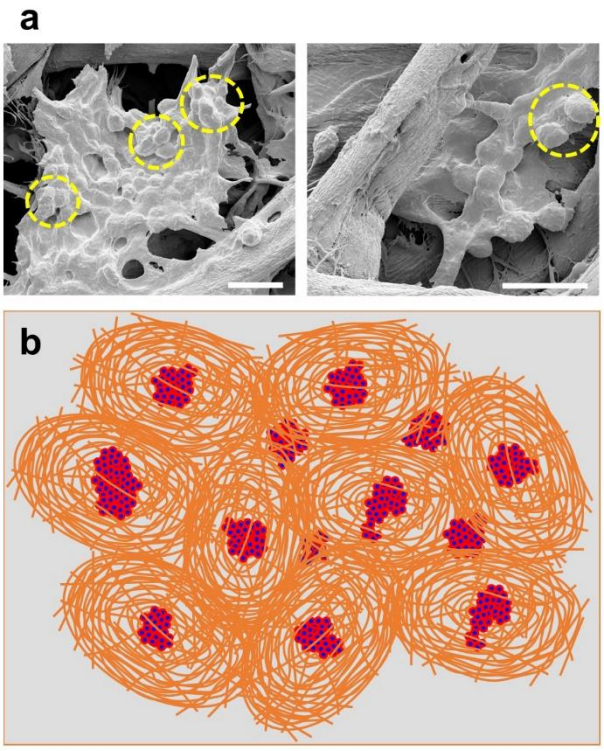

Figure S7. Interconnecting fibers in conjunction to the growth of spheroids. (a) SEM images reveal the existence of post-cryopreserved cells within the paper pores, wherein they seemingly act as connecting bridges between the paper fibers. Example cell clusters (dashed yellow circles) are clearly distinguishable among them. Scale bars are 25 µm. (b) Schematic representation of the interconnecting fibers (orange) within paper that supposedly serve as nests to support the growth of 3D spheroids (blue = nucleus and red = F-actin) within a paper following their cryopreservation.

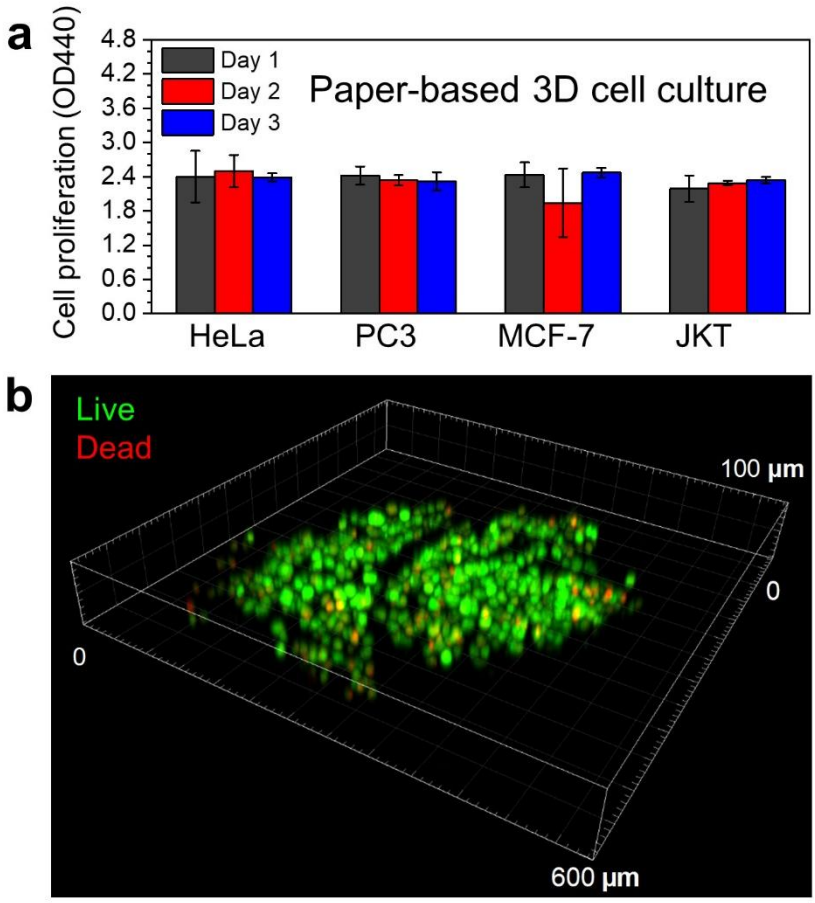

Figure S8. Examination of proliferation and survival of cells in paper-based 3D culture. (a) Proliferation study reveals that HeLa, PC3, MCF-7, and JKT cells within paper platforms show growth. Values and error bars represent mean ± S.D. ($n \geq 3$). (b) Following 7 days of 3D paper-based HeLa cell culture, freezing for 2 days at -80 ºC, and finally thawing; experiments showed integrity and survival of cells.